

# Electrical properties of amorphous SiC<sub>x</sub>N<sub>y</sub>H<sub>z</sub>-ceramics derived from polyvinylsilazane

Stephan Trassl<sup>a</sup>, Manfred Puchinger<sup>a,1</sup>, Ernst Rössler<sup>b,\*</sup>, Günter Ziegler<sup>a</sup>

<sup>a</sup>*Institute for Materials Research (IMA I), University of Bayreuth, 95440 Bayreuth, Germany*

<sup>b</sup>*Institute of Physics (EP II), University of Bayreuth, 95440 Bayreuth, Germany*

Received 20 October 2001; received in revised form 27 March 2002; accepted 28 April 2002

## Abstract

Electrical properties of monolithic, amorphous SiC<sub>x</sub>N<sub>y</sub>H<sub>z</sub>-ceramics derived from 1,3,5-trimethyl-1,3,5-trivinylcyclotrisilazane via polymer pyrolysis were investigated from room temperature to 400 °C using impedance spectroscopy. Depending on the pyrolysis temperature  $T_p$ , the d.c. conductivity varies up to 8 orders of magnitude. The temperature dependence of samples pyrolysed at low temperatures ( $T_p = 700\text{--}1200$  °C) follows a Mott law, whereas samples pyrolysed at high temperature ( $T_p = 1400$  °C) show an Arrhenius dependence. Structural changes during pyrolysis were characterized by solid state magic angle spinning nuclear magnetic resonance spectroscopy, Raman spectroscopy and X-ray diffractometry. NMR and especially Raman measurements indicate the formation of sp<sup>2</sup>-carbon atoms, which rearrange towards graphitic-like domains with increasing pyrolysis temperature. This observation can explain the related increase of the d.c.-conductivity.

© 2002 Elsevier Science Ltd. All rights reserved.

**Keywords:** Amorphous materials; Electrical conductivity; Precursors-organic; SiCN; Silicon carbonitrides; Structural characterization

## 1. Introduction

The use of organometallic compounds as precursors of amorphous ceramics has attracted wide interest since the pioneering work of Verbeek and Winter<sup>1</sup> as well as Yajima<sup>2</sup> in the 1970s. An essential impulse for the work in the field of precursor-derived ceramics evolved from the search for materials with high temperature stability. The non-oxidic binary, ternary and quaternary systems Si–C, Si–C–N and Si–C–B–N, respectively, have attracted most of the recent attention. Besides the promising high-temperature properties in the amorphous state, the processing route offers the possibility to prepare ceramic powders, binders, fibers, coatings and ceramic matrix composites (CMCs). The SiCN-ceramics obtained via the pyrolysis of organometallic compounds exhibit excellent thermo-mechanical properties in comparison with conventionally processed (powder route) Si<sub>3</sub>N<sub>4</sub> and

SiC due to the low impurity level and the homogeneous element distribution.

Despite their importance for engineering applications the electrical properties of amorphous precursor-derived ceramics have hardly been investigated so far. Mocaer et al.<sup>3</sup> first carried out measurements of the d.c.-conductivity of polysilazane-derived ceramics. Haluschka et al.<sup>4</sup> studied the d.c.- and a.c.-conductivity of ceramics in the Si–C–N system in detail. The d.c.-conductivity of pyrolysed polyvinylsilazane was examined by Eins et al.<sup>5</sup> All of them observed semiconducting properties and a strong increase of the d.c.-conductivity as a function of pyrolysis temperature ( $T_p$ ). Mocaer et al. explain the changes in the d.c.-conductivity and in its temperature dependence during pyrolysis with the growth of dehydrogenated aromatic carbon and its local arrangement as cage-like structures around SiC-crystallites. The underlying conducting mechanism is given as hopping process of the charge carriers between the more or less complete interconnected cages of carbon. Haluschka et al., who studied the conductivity of SiCN-ceramics pyrolysed in the temperature region between 1000 and 1700 °C, divided the results in three temperature regimes. In the first regime between 1000 and 1300 °C the material is still amorphous and shows a semiconducting behavior

\* Corresponding author. Tel.: +49-921-55-2606; fax: +49-921-55-2621.

E-mail address: ernst.rossler@uni-bayreuth.de (E. Rössler).

<sup>1</sup> Present address: Max-Planck-Institut für Metallforschung, Seestr. 92, 70174 Stuttgart, Germany.

with a  $T^{-1/4}$  dependence of  $\sigma_{dc}$ . Haluschka et al.<sup>4</sup> presume that the tunneling of large polarons is the main transport mechanism in this regime. They explain the increase of the d.c.-conductivity for  $1000\text{ }^\circ\text{C} < T_p < 1300\text{ }^\circ\text{C}$  with an enhanced  $sp^2$ -/ $sp^3$ -ratio of the carbon atoms. In the second regime for  $T_p = 1300\text{--}1600\text{ }^\circ\text{C}$  the authors reported that nano-crystalline SiC particles arise, which are responsible for the increase of  $\sigma_{dc}$  by formation of percolation paths throughout the sample. Finally, beyond  $T_p = 1600\text{ }^\circ\text{C}$ , when the samples are completely crystalline, the electric conductivity of nitrogen doped  $\beta$ -SiC is found.

This paper presents electrical conductivity measurements on amorphous  $\text{SiC}_x\text{N}_y\text{H}_z$ -ceramics derived from 1,3,5-trimethyl-1,3,5-trivinylcyclotrisilazane ([MeViSiNH]<sub>3</sub>, VN) between room temperature and  $400\text{ }^\circ\text{C}$ . Our objective here is to study the correlation between the microstructure of the SiCN-ceramics, especially of the free carbon phase formed during pyrolysis and the d.c.- as well as the a.c.-conductivity. For this work, VN was crosslinked and pyrolysed at different temperatures in order to investigate the electrical properties and the structural characteristics of the received amorphous  $\text{SiC}_x\text{N}_y\text{H}_z$ -ceramic compact. Structural information was obtained by solid state magic angle spinning nuclear magnetic resonance spectroscopy (MAS-NMR), Raman spectroscopy (RS) and X-ray diffraction (XRD). Impedance spectroscopy was employed to investigate the electrical properties in the frequency range  $10^{-2}\text{--}10^7\text{ Hz}$ . The correlation of the electrical behavior with the structural changes during pyrolysis is of special importance for an intentional modification or even the tailoring of properties of this class of material.

## 2. Experimental procedure

### 2.1. Material

Methylvinylchlorosilane was brought to reaction with  $\text{NH}_3$  as reported by Lücke et al.<sup>6</sup> The compound [MeViSiNH]<sub>3</sub> (VN) in the received solution was distilled off and used as the precursor ( $\eta = 1.8 \pm 0.3 \cdot 10^{-3}\text{ Pa s}$ ,  $\rho = 940\text{ kg/m}^3$ ).

The silazane was crosslinked by using dicumylperoxide (DCP) as radical initiator and subsequent thermal treatment at  $300\text{ }^\circ\text{C}$  for 3 h in  $\text{N}_2$ -atmosphere. Powder of the crosslinked precursor was obtained from the as-received unmeltable solid using a ball mill and zirconia milling media. The powder was sieved and the fraction  $< 63\text{ }\mu\text{m}$  was used to produce compacts. For this purpose the crosslinked powder particles were blended with 30 vol.% binder consisting of the liquid precursor VN mixed with 2 wt.% DCP. The added precursor acts both for filling of the pores in the green compact and as a reactive component causing coalescence of the powder

particles. Due to the low self-diffusion coefficient of the atoms, this is a suitable possibility to guarantee a homogeneous dense compact. Uniaxial pressing at  $7.5\text{ MPa}$  of the powder-binder mixture and subsequent annealing at  $500\text{ }^\circ\text{C}$  for 5 h to crosslink the liquid precursor acting as a binder between the powder particles yields a monolithic green body with a porosity of about 48%. This intermediate product was infiltrated once again with the liquid binder under reduced atmosphere ( $0.1\text{ mbar}$ ). After repeating the infiltration and the thermal treatment two times the porosity decreased to about 32%.

In order to determine the electrical properties, the samples were cut and abraded to provide a defined geometrical shape (rectangular solids, circa  $10 \times 3 \times 1.5\text{ mm}$ ). Subsequently, the final pyrolysis was performed at various temperatures ranging from  $600\text{ to }1400\text{ }^\circ\text{C}$  in  $\text{N}_2$ -atmosphere for 5 h. For impedance spectroscopy the samples have to be coated with a metal film. For this purpose a silver suspension was spread on both ( $10 \times 3\text{ mm}$ )-faces of the compacts, and in order to improve the contact between the sample and the silver coating the compact was annealed once again at  $400\text{ }^\circ\text{C}$  for 1 h.

### 2.2. Methods of characterization

For structural characterization, the compacts were ground.  $^{13}\text{C}$  and  $^{29}\text{Si}$  NMR spectra of the solid intermediates between  $300\text{ and }1600\text{ }^\circ\text{C}$  were obtained on a Bruker AVANCE DSX 400 spectrometer applying the magic angle spinning technique (MAS) with spinning rates  $5\text{--}7\text{ kHz}$ . For preparation temperatures ( $T_p$ ) up to  $700\text{ }^\circ\text{C}$ , a signal to noise enhancement using the cross polarisation (CP) method was possible due to the presence of a sufficient amount of protons in the samples. For compacts heated above  $700\text{ }^\circ\text{C}$ , the CP method became inefficient since the proton concentration became too low. Therefore single pulse excitation was employed for recording  $^{29}\text{Si}$  spectra in the latter case.  $^{13}\text{C}$  spectra were recorded with a depth pulse excitation, in this case ( $T_p > 700\text{ }^\circ\text{C}$ ), in order to avoid the  $^{13}\text{C}$  signal from the sample holder. The chemical shift data in the  $^{13}\text{C}$  and  $^{29}\text{Si}$  NMR spectra are listed with respect to tetramethylsilane (TMS) as an external standard.

Raman spectra were acquired on a Bruker FRA 106. Potassium bromide (KBr)-pellets of the samples were excited in backscattering geometry using a probe wavelength of  $1064\text{ nm}$ . For the analysis of crystalline phases in the pyrolytic residues above  $1000\text{ }^\circ\text{C}$ , X-ray diffraction (XRD) studies were carried out on a Seifert XRD 3000 P powder diffractometer using  $\text{CuK}_\alpha$  radiation. Additional microstructure characterization was performed by transmission electron microscopy (TEM), employing a Philips CM20FEG (field emission gun) microscope. TEM-foil preparation followed standard techniques involving diamond cutting, ultra-sound

drilling, mechanical grinding, dimpling, Ar-ion thinning to perforation and subsequent light carbon coating to minimise electrostatic charging under the electron beam. The probe size used in this study was about 5 nm in diameter. Mass change during pyrolysis was investigated with a Netzsch STA 409 thermobalance linked with an FTIR analysis unit (Bruker FRA 106).

The electric properties of the compacts were measured employing impedance spectroscopy. The experiments were performed using a frequency response analyzer (SI 1260) in connection with a current-to-voltage converter (Novocontrol;  $10^{-2}$ – $10^7$  Hz) and a home-built sample holder enabling measurements in the temperature range from room temperature to about 400 °C under inert atmospheres. Two samples of each temperature of pyrolysis were measured at a step width of 50 K. The sample coated with silver was inserted between silver electrodes and the complex impedance  $\hat{Z}(\omega) = z' + iz''$  of the compacts was determined. The complex conductivity  $\hat{\sigma}(\omega)$  and the complex dielectric constant  $\hat{\epsilon}_r(\omega)$  can be derived from  $\hat{Z}(\omega)$  [7],

$$\hat{\sigma}(\omega) = \frac{1}{\frac{A}{d} |\hat{Z}|^2} \cdot (z' - iz'') \quad (1)$$

$$\hat{\epsilon}_r(\omega) = \frac{1}{\omega \epsilon_0 \frac{A}{d} |\hat{Z}|^2} \cdot (-z'' - iz') \quad (2)$$

where  $A$  is the area of the plate capacitor (10×3 mm) and  $d$  the distance of the plates (1.5 mm).

The d.c. conductivity was measured by determining the low frequency limit ( $\nu < 0.1$  Hz) of the real part of the conductivity (cf. Fig. 4a):

$$\sigma'(\omega, T) = \sigma_{dc}(T) + \sigma'_{ac}(\omega, T) \quad (3)$$

The error of the  $\hat{\sigma}(\omega)$  data obtained from these measurements is about 50%.

All spectroscopic, microscopic and XRD experiments were carried out at room temperature (RT).

### 3. Results

#### 3.1. Structural characterization

During the first step of heat treatment catalytic crosslinking of the liquid precursor VN mixed with 2 wt.% DCP takes place at about 120 °C via the polymerization of the vinyl-groups. The liquid precursor converts into a pale yellow solid. Further heating ( $T_p = 300$ – $750$  °C) causes the transformation of the crosslinked precursor into the amorphous  $\text{SiC}_x\text{N}_y\text{H}_z$  ceramic. During pyrolysis the color of the material

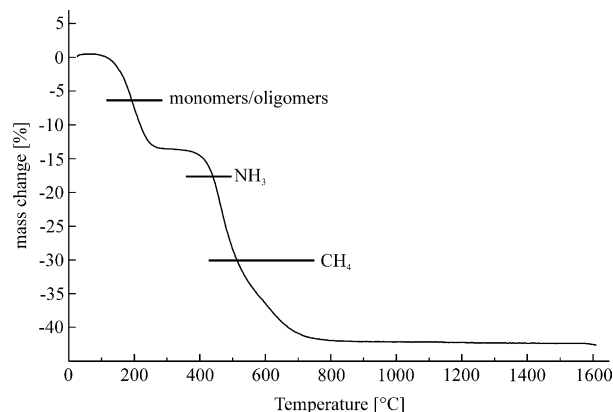


Fig. 1. TG analysis coupled with simultaneous FTIR spectroscopy of gaseous species forming during pyrolysis of the precursor VN.

changes from pale yellow to brown and finally black. A two step mass change is involved with the ceramization of the precursor VN (Fig. 1). Between 120 and 300 °C the first mass loss is about 14 wt.%, owing to the release of gaseous oligomers, as identified by coupled TG-FTIR measurements. A second stage of mass loss is observed between 380 and 750 °C, where ammonia and methane are released, which indicates the degradation of the organic substituents. Above 800 °C, no significant mass changes can be observed any longer.

Changes in the structure of the solid intermediates during thermal treatment at temperatures beyond 300 °C were investigated by  $^{29}\text{Si}$  and  $^{13}\text{C}$  solid state NMR spectroscopy. Fig. 2a ( $^{29}\text{Si}$ ) and b ( $^{13}\text{C}$ ) shows the room temperature NMR spectra of the system VN for different pyrolysis temperatures  $T_p$ . In the  $^{29}\text{Si}$  NMR spectrum for  $T_p = 300$  °C, a strong peak at  $-2.8$  ppm is observed in addition to another one at  $-15$  ppm caused by unreacted  $(\text{N})_2\text{Si}(\text{CH}_3)\text{CH}=\text{CH}_2$  sites. In addition to the sharp line of the silylmethyl- ( $4.2$  ppm) and the double peak of the silylvinyl-group ( $132/141$  ppm) of the precursor, the  $^{13}\text{C}$  NMR spectrum shows one broad line at about 28 ppm. Since the crosslinking of VN takes place via the polymerization of vinyl-groups, the resonance at 28 ppm in the  $^{13}\text{C}$  spectrum and at  $-2.8$  ppm in the  $^{29}\text{Si}$  spectrum can be assigned to this reaction yielding  $(\text{N})_2(\text{CH}_3)\text{Si}-(\text{CH}-\text{CH}_2)_n$  sites.<sup>8</sup> Further heating causes the broadening of all  $^{29}\text{Si}$ -NMR lines. For  $T_p = 500$  °C, the peaks assigned to the vinyl-group and the resonance at 28 ppm in the  $^{13}\text{C}$  spectrum due to the formation of aliphatic carbon atoms during the polymerization have disappeared. Heating above 500 °C causes the appearance of a new signal in the  $^{13}\text{C}$  spectrum at 135 ppm, which increases in intensity at 700 °C. Coincidentally, a high-field shift (shift towards lower chemical shift values) of the signals in the  $^{29}\text{Si}$  spectra takes place corresponding to an increase of the number of Si–N bonds and a decrease of the number of Si–C bonds, probably due to both the formation of C-containing gas

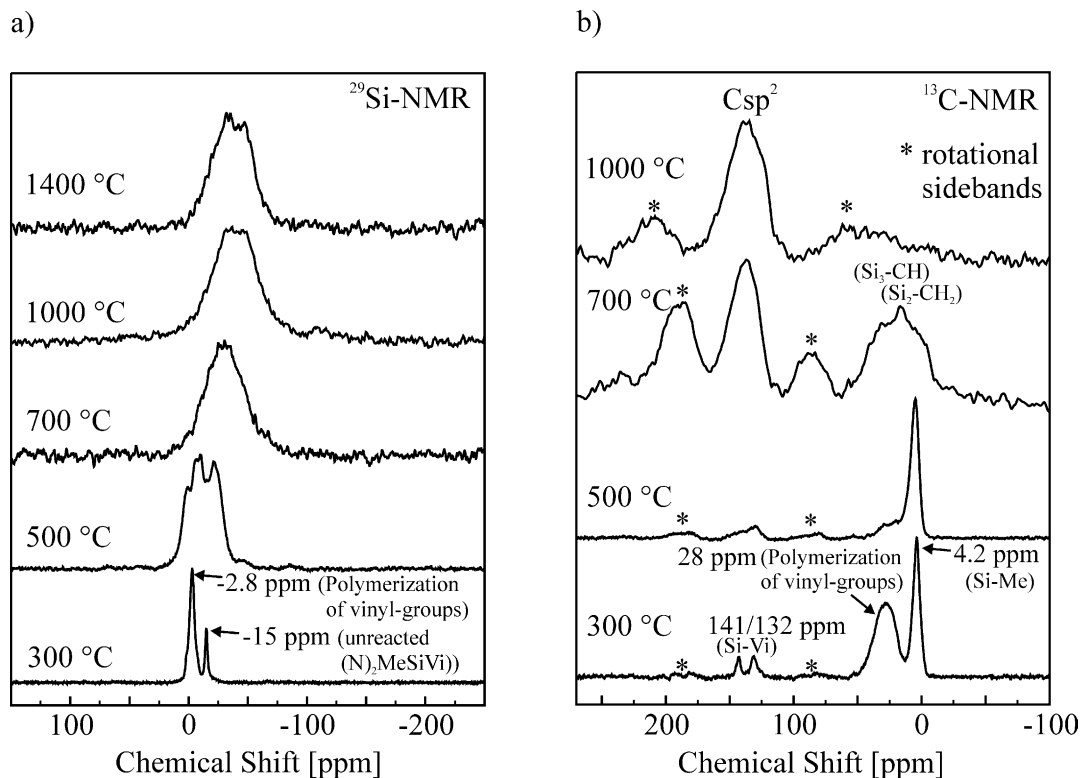


Fig. 2. (a)  $^{29}\text{Si}$ - and (b)  $^{13}\text{C}$ -NMR spectra of VN-derived powder samples heat treated at various temperatures  $T_p$ . ( $^{13}\text{C}$ -NMR: 300–700 °C: spinning speed 5 kHz, 1000 °C: spinning speed 7 kHz.)

species ( $\text{CH}_4$ ) and the segregation of carbon clusters. The signal at 135 ppm in the  $^{13}\text{C}$  NMR spectra, which is characterized by a broad chemical shift tensor causing strong rotational sidebands, indicates a high amount of  $\text{sp}^2$ -carbon in the form of clusters, the so called free carbon.<sup>9,10</sup> Pyrolysis at 1400 °C finally yields an amorphous ceramic composed of a free carbon phase and a  $\text{SiC}_x\text{N}_y$  phase. X-ray analysis of powder specimen from the whole temperature range ( $T_p = 600$ –1400 °C) showed no crystalline phases.

Raman spectroscopy was used to characterize the modification of the free carbon. Fig. 3 shows the Raman spectra for different  $T_p$ . For  $T_p > 850$  °C, two Raman bands are observed at wave numbers of 1280 and 1600  $\text{cm}^{-1}$ , which are allocated to the D and G band, respectively, and are the two most prominent features of disordered graphitic-like  $\text{sp}^2$ -carbon.<sup>11,12</sup> This indicates carbon segregation as disordered or nano-crystalline graphitic clusters. Since the line widths decrease with increasing pyrolysis temperature, structural rearrangements accompanied by ordering of the free carbon phase occur for  $1000$  °C  $< T_p < 1400$  °C.

### 3.2. Electrical properties

Measurements of the complex conductivity of the samples are limited in frequency due to the electronics of the experimental setup. While the determination of

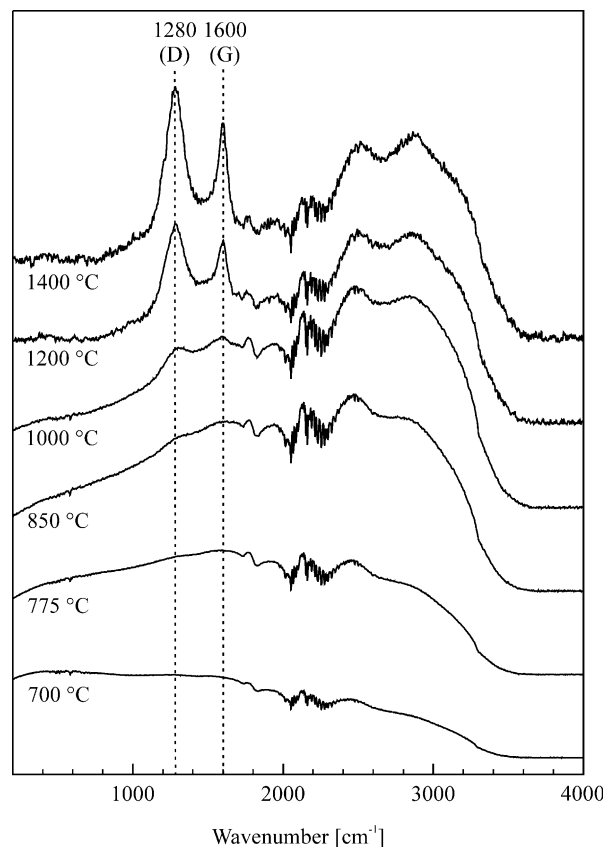


Fig. 3. Raman spectra of pyrolytic residues of the precursor VN annealed at temperatures  $T_p$  between 700 and 1400 °C.

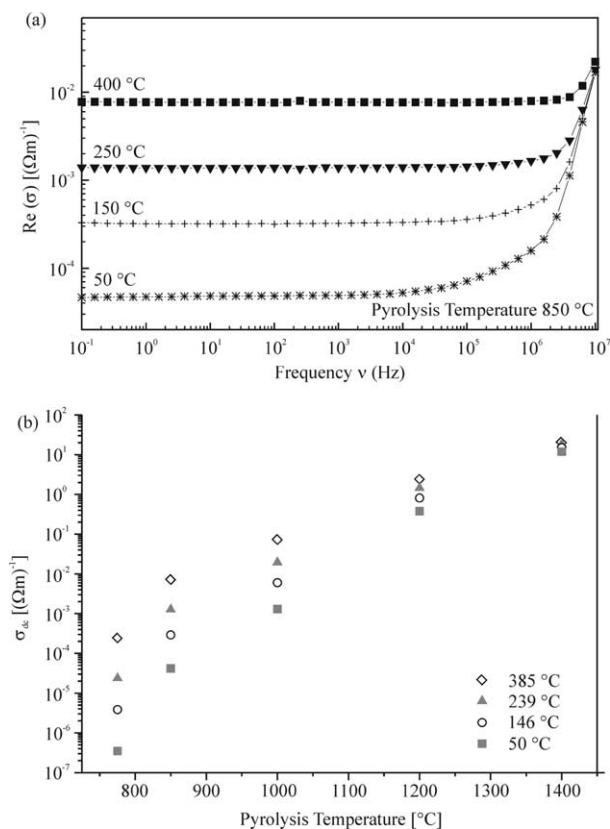


Fig. 4. (a) Real part of the conductivity of VN-ceramic heat treated at 850 °C depending on the measuring temperature. (b) Received d.c.-conductivity of VN-ceramic at different pyrolysis temperatures depending on the measuring temperature.

the real part of the conductivity  $\sigma'(\omega)$  was possible for samples pyrolysed above 700 °C over the whole frequency ( $10^{-1}$ – $10^6$  Hz) and temperature range (RT–400 °C), the imaginary part of the conductivity was only obtained in the case of low pyrolysis temperatures and high frequencies.

### 3.2.1. d.c.-Conductivity

Measurement of the d.c.-conductivity was carried out via the determination of the real part of the conductivity at low frequencies ( $\sigma_{dc} = \sigma'(\nu = 0.1 \text{ Hz})$ ). In Fig. 4a  $\sigma'(\omega)$  is plotted for the sample pyrolysed at 850 °C for different measuring temperatures. The received d.c.-conductivity depends on the temperature and is shown for selected samples as a function of heat treatment in terms of  $T_p$  in Fig. 4b. All samples show an increase of  $\sigma_{dc}$  with rising temperature. Therefore, these  $\text{SiC}_x\text{N}_y\text{H}_z$ -ceramics can be regarded as amorphous semiconductors. At low pyrolysis temperatures ( $T_p = 775$  °C), the temperature dependence of  $\sigma_{dc}$  is strong causing a variation of about 3 orders of magnitude. In contrast, at high pyrolysis temperatures ( $T_p = 1400$  °C) the d.c.-conductivity changes only by a factor of 2. As depicted in Fig. 4b, we also find an increase of the d.c.-conductivity

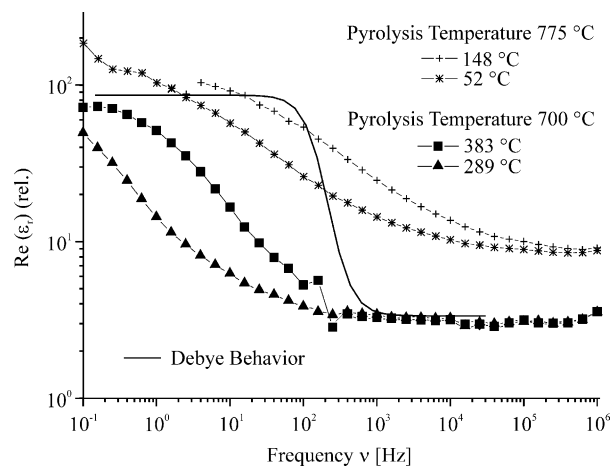


Fig. 5. Real part of the relative permittivity as function of the frequency  $\nu$  depending on the measuring temperature for  $T_p = 700, 775$  °C.

of up to 8 orders of magnitude as a function of heat treatment ( $T = 50$  °C).

### 3.2.2. a.c.-Conductivity

The real part of the a.c.-conductivity is obscured by the d.c.-conductivity and, therefore, can only be obtained, if the d.c.-conductivity is at most by one order of magnitude higher than the real part of the a.c.-conductivity. For our samples, this is only the case at low pyrolysis and measurement temperatures as well as at high frequencies  $\nu$ . The imaginary part of the a.c.-conductivity is equivalent to the real part of the relative permittivity  $\epsilon'_r(\nu)$ , explicitly  $\sigma''(\nu) = \mu \cdot \epsilon'_r(\nu)$ . In the measurable range,  $\epsilon'_r(\nu)$  varies between 5 and 180. Low values were obtained in the case of high frequencies  $\nu$  and low pyrolysis temperatures. Plotting  $\log(\epsilon'_r(\nu))$  vs  $\log(\nu)$  (Fig. 5) we found a step-like behavior typical of a relaxation process passing through the accessible frequency window. This relaxation process is very broad in contrast to a Debye behavior.

## 4. Discussion

### 4.1. Correlation between structure and d.c.-conductivity

According to Heywang,<sup>13</sup> the temperature dependence of the d.c.-conductivity  $\sigma_{dc}$  of amorphous semiconductors can be described as follows. In the case  $kT < E_{\text{gap}}$  ( $k$ : Boltzmann constant,  $E_{\text{gap}}$ : energy gap between Fermi level and conducting band),  $\sigma_{dc}(T)$  follows the Mott law:

$$\sigma_{dc}(T) = \sigma_0 \exp \left[ - \left( \frac{T_0}{T} \right)^{\frac{1}{4}} \right] \quad (4)$$

Although other mechanisms of conduction have been proposed,<sup>14</sup> variable range hopping is supposed to be

the explanation for this temperature behavior (4).<sup>15</sup> Variable range hopping means single-phonon-assisted jumps of charge carriers near the Fermi level. Multi-phonon-assisted jumps, however, lead to the same kind of temperature dependence.<sup>16</sup>

In the case  $kT \gg E_{\text{gap}}$ , charge carriers in the conducting band determines the temperature dependence of the d.c.-conductivity and an Arrhenius behavior follows,

$$\sigma_{\text{dc}}(T) = \sigma_0 \exp\left[-\left(\frac{\Delta E}{kT}\right)\right] \quad (5)$$

where  $\Delta E$  is the activation energy (energy gap between Fermi level and conducting band).

In order to get information on the conducting mechanism, the correspondence between the experimental data and Eqs. (4) and (5) was tested. Data analysis revealed a good agreement with the Mott law for samples pyrolysed at temperatures between 775 and 1200 °C, although deviations increase at 1200 °C (Fig. 6a). For  $T_p > 1200$  °C, however, the Arrhenius behavior fits the experimental data better than the first one (Fig. 6b). The change of the temperature dependence of the d.c.-conductivity of the samples during

annealing between 775 and 1400 °C indicates a decrease of the energy gap  $E_{\text{gap}}$  with increasing pyrolysis temperature. This is in agreement with the values of  $\Delta E$  determined from experimental data using Eq. (5) (Fig. 6c).  $\Delta E$  decreases from about 0.7 eV at low pyrolysis temperature ( $T_p = 700$  °C) to about 30 meV for  $T_p = 1400$  °C. The former value of  $\Delta E$  is high in comparison with  $kT$  in the temperature range between room temperature RT and 400 °C, and it is on the typical scale of the energy gap of crystalline semiconductors (Si:  $\Delta E = 1.1$  eV). However, the latter value of  $\Delta E$  is of the order of magnitude of  $kT$  and excludes the low-temperature approximation for variable-range-hopping. Therefore, the change of the temperature dependence of the d.c.-conductivity suggests the following explanation: At low pyrolysis temperatures,  $E_{\text{gap}} > kT$  is valid. The d.c.-conductivity is properly described by a Mott law indicating a transport mechanism via variable-range-hopping. At higher pyrolysis temperatures ( $1200$  °C  $< T_p < 1400$  °C),  $E_{\text{gap}} > kT$  is no longer valid. That means, samples pyrolysed at 1400 °C behave different from the preceding ones. Furthermore, the values of  $\sigma_{\text{dc}}$  in this temperature range are very high for an amorphous semiconductor. So a smaller energy gap and charge carriers in the conducting band must be assumed.

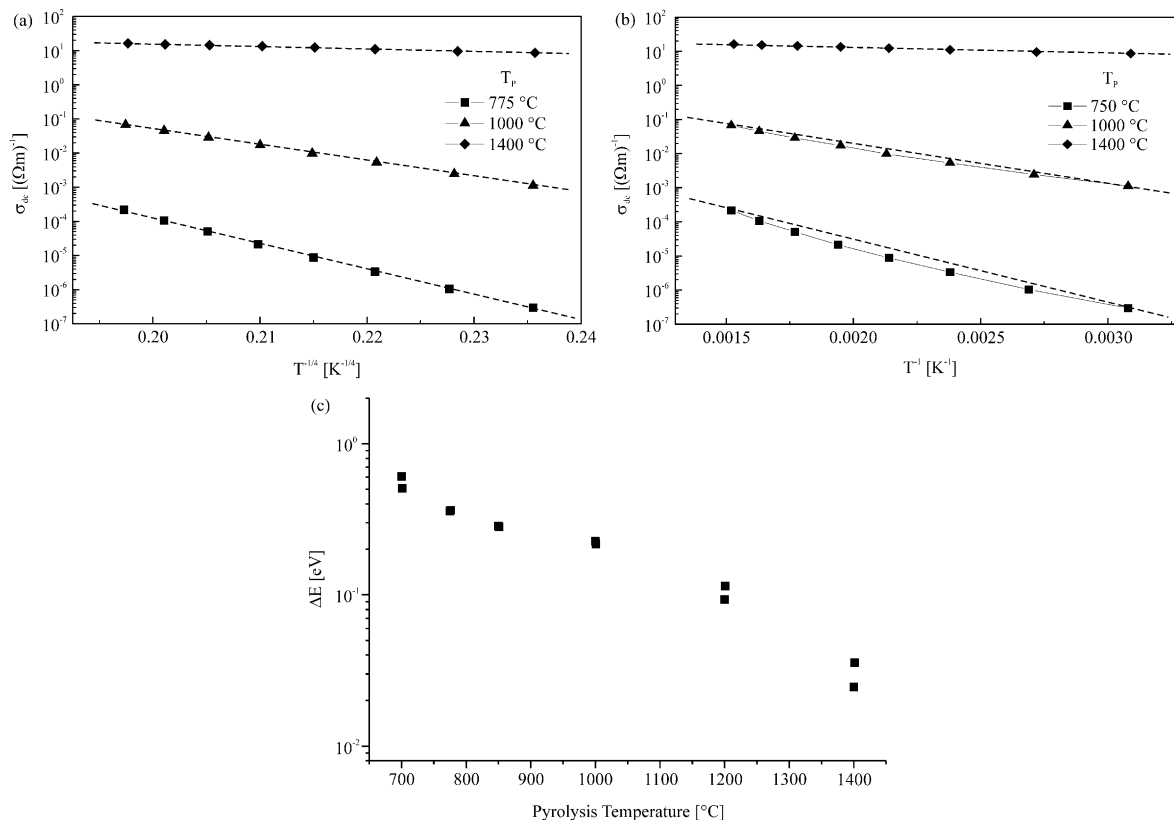


Fig. 6. Temperature dependence of d.c.-conductivity of VN-derived ceramics heat treated at various temperatures. (a) Plotting  $\log(\sigma_{\text{dc}})$  versus  $T^{-1/4}$  (Mott law) reveal a good agreement for samples pyrolysed at temperatures between 775 and 1200 °C. (b) Plotting  $\log(\sigma_{\text{dc}})$  versus  $T^{-1}$  (Arrhenius law) reveal a good agreement for samples pyrolysed at temperatures above 1200 °C. (c) Activation energies of the d.c.-conductivity of VN-derived ceramic at different pyrolysis temperatures. For the calculation a Boltzmann dependency of  $\sigma_{\text{dc}}(T)$  is assumed.

Table 1  
d.c.-Conductivity and chemical composition of different SiCN-ceramics

Material ( $T_p$ )	Chemical composition	Estimated phase composition	Amount of $C_{\text{free}}$ (mol%)	$\sigma_{\text{dc}}$ [ $(\Omega\text{m})^{-1}$ ] at RT
NCP 200 (1050 °C) <sup>a</sup>	$\text{SiN}_{0.88}\text{C}_{0.59}$	1 $\text{Si}_3\text{N}_4$ + 1.53 SiC + 1.14 C	31	$10^{-7}$
VN (1000 °C)	$\text{SiN}_{0.73}\text{C}_{1.46}$	1 $\text{Si}_3\text{N}_4$ + 2.48 SiC + 5.52 C	61	$10^{-3}$
VT 50 (1050 °C) <sup>b</sup>	$\text{SiN}_{1.5}\text{C}_{2.0}$	1 $\text{Si}_3\text{N}_4$ + 0.5 N + 6.0 C	80	$10^{-2}$

<sup>a</sup> From Ref. [4].

<sup>b</sup> From Ref. [5].

An appearance of a graphitic-like  $\text{sp}^2$ -carbon phase at higher pyrolysis temperatures may explain both the increase of the d.c.-conductivity and the change of the temperature dependence of  $\sigma_{\text{dc}}(T)$ . Graphite is a semi-metal and, therefore, shows no energy gap between valence band and conducting band. The formation of a graphitic carbon phase leads to a high density of states within the mobility gap of the amorphous semiconductor and, thus, the effective energy gap between valence band and conducting band is reduced. If the content of the graphitic carbon phase reaches the percolation threshold, the electrical properties of the material can be dominated by this phase.<sup>17</sup> Both homogeneous distribution of carbon clusters or a network of graphitic-like lamellae of a few atom layers in size can be assumed. The former model has a relatively high percolation threshold of about 16 vol.%. In the latter case, however, a very small volume fraction of a highly conducting carbon phase is able to alter the electrical conductivity completely. The latter model, consisting of a network of graphitic-like lamellae, is equal to the suggested structure of glassy carbon.

NMR and Raman results indicate the formation of a graphitic-like  $\text{sp}^2$ -carbon phase, too. In the  $^{13}\text{C}$ -NMR spectra a signal corresponding to  $\text{sp}^2$ -carbon is observed. The appearance of the D and the G band at about 1280 and 1600  $\text{cm}^{-1}$ , respectively, in the Raman spectra of the ceramic material indicates carbon segregation as disordered or nano-crystalline graphitic-like carbon. The Raman spectrum of the sample heated to 1400 °C is similar to that of glassy carbon.<sup>18</sup> The line widths of both the G band and the D band decrease and the intensity ratio (D:G) of the two bands slightly rises with increasing pyrolysis temperature. At low domain sizes (up to 2 nm) this intensity ratio is inversely proportional to the domain size of nano-crystalline graphite<sup>19</sup> and the value of  $I_{\text{D}}:I_{\text{G}} = 3.0$  for  $T_p = 1400$  °C corresponds to an average size of about 1.5 nm. This analysis suggests structural rearrangements in the carbon phase through either an increased number of crystallites and/or an increase in size and ordering of existing nano-crystallites.

No excess carbon phase could be imaged by HRTEM upon annealing at temperatures as high as 1400 °C, which is at first glance inconsistent with the results

obtained from Raman spectroscopy. The finding that the excess free carbon phase was not visible under optimized electron optical conditions for high-resolution imaging implies two consequences: (i) the carbon phase is not well ordered (amorphous-like) and hence gives a similar projected potential as the surrounding amorphous SiCN-matrix and/or (ii) the ordered carbon regions are considerably smaller than the foil thickness (10–20 nm) illuminated by the electron beam. In the latter case, the presence of well ordered graphitic inclusions would not necessarily be seen in the HRTEM image, because these small regions are embedded within an amorphous matrix being 10–20 times larger in thickness than the inclusions themselves. Indeed, from Raman measurements it was estimated, that the graphitic regions in the samples are only  $\sim 1.5$  nm in size.

In Table 1 the d.c.-conductivity of VN is compared to results of earlier works of Haluschka<sup>4</sup> and Eins.<sup>5</sup> In general, all amorphous SiCN-ceramics investigated in these papers show semiconducting behavior and an increase of the d.c.-conductivity of some orders of magnitude with increasing annealing temperature as in the present paper. The authors explain the increase of the absolute electrical conductivity as well as the change of the temperature dependence with the formation of unsaturated carbon. Comparing the d.c.-conductivity and the chemical composition of VN-derived ceramics with those values for the ceramic materials received from pyrolysis of commercially available NCP 200<sup>4</sup> and VT 50,<sup>5</sup> respectively (cf. Table 1), one gets higher d.c.-conductivity for materials with higher amount of free carbon. A similar correlation between electrical conductivity and free carbon content was also observed by Trassl et al.<sup>10</sup>

To summarize, the formation of a  $\text{sp}^2$ -carbon phase and its structural rearrangements in connection with an increasing degree of order may explain both the results obtained by the electrical conductivity measurements and by the structural characterization.

#### 4.2. Dielectric relaxation

At pyrolysis temperatures between 700 and 775 °C, we observed a frequency dependence of  $\epsilon'_r(\nu)$  which is typical of a relaxation process passing through the

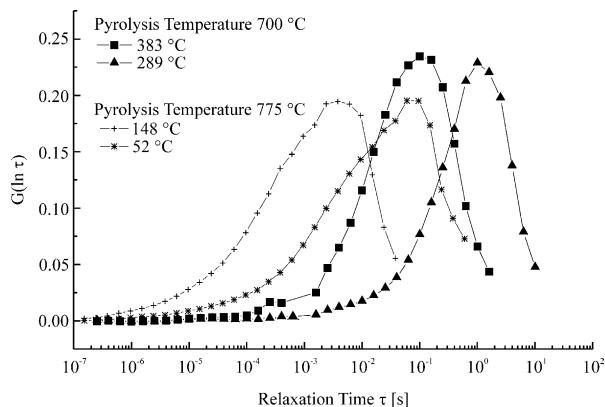


Fig. 7. Distribution of relaxation times depending on the measuring temperature for  $T_p = 700, 775$  °C.

experimental window (cf. Fig. 5). This behavior may be characterized by a distribution of relaxation times  $G(\ln\tau)$  and the complex dielectric susceptibility  $\chi(\omega)$  can be described,<sup>7</sup>

$$\chi(\omega) = \chi_0 \cdot \int_{\tau=0}^{\infty} \frac{G(\ln\tau)}{1 + i\omega\tau} d(\ln\tau) \quad (6)$$

where  $\chi_0$  is the static susceptibility. In the case of a very broad distribution (cf. Fig. 5)  $G(\ln\tau)$  can be estimated from  $\varepsilon'_r(\nu)$  using the approximation formula:<sup>7</sup>

$$G\left(\ln \frac{1}{\omega}\right) \sim - \frac{1}{\Delta\varepsilon} \frac{d\varepsilon'(\omega)}{d(\ln\omega)} \quad (7)$$

The results are shown in Fig. 7. We found relaxation times in the range of seconds. Shorter relaxation times were found for higher measuring temperatures and higher pyrolysis temperatures. These tendencies were also observed by Haluschka et al.<sup>4</sup> Relaxation times in the order of seconds are relatively long for an electronic process, and a correlation with long-living trap states within the mobility gap of the amorphous semiconductor is likely. These localized trap states evolve from deviations from the perfect amorphous structure, i. e. the structure having just the minimum of distortions of bonding angles and the narrowest possible distribution of bond lengths. A higher pyrolysis temperature provides a higher mobility of the atoms, so rearrangements and optimization of the amorphous structure becomes possible. This means the amount of trap states can be reduced at higher pyrolysis temperatures, and thus the effective relaxation time decreases.

## 5. Conclusion

Pyrolysis of 1,3,5-trimethyl-1,3,5-trivinylcyclotrisilazane ([MeViSiNH]<sub>3</sub> (VN)) under nitrogen atmosphere led to monolithic, amorphous SiC<sub>x</sub>N<sub>y</sub>H<sub>z</sub>-ceramics.

Impedance spectroscopy was used to investigate the electrical properties of the monolithic SiCN-ceramic as a function of temperature for different pyrolysis procedure. The d.c.-conductivity  $\sigma_{dc}$  measured at 50 °C increases about 8 orders of magnitude from  $10^{-7}$  ( $\Omega\text{m}$ )<sup>-1</sup> ( $T_p = 775$  °C) to  $10^1$  ( $\Omega\text{m}$ )<sup>-1</sup> ( $T_p = 1400$  °C). The samples show semiconducting behavior. At low pyrolysis temperatures ( $T_p \leq 1000$  °C), the temperature dependence of the d.c.-conductivity  $\sigma_{dc}$  follows a Mott-law ( $\sigma_{dc} \sim \exp(T^{-1/4})$ ) (variable-range-hopping). At higher pyrolysis temperatures ( $1200$  °C  $\leq T_p \leq 1400$  °C), the temperature dependence of the d.c.-conductivity  $\sigma_{dc}$  can be described by an Arrhenius law.

NMR and especially Raman results suggest the formation of a graphitic-like sp<sup>2</sup>-carbon phase. The appearance of such a carbon phase and its structural rearrangements can explain the observed electrical behavior.

The real part of the relative permittivity varies between 5 and 180 obtaining low values in the case of high frequencies  $\nu$  and low pyrolysis temperatures. We found a step-like behavior typical of a relaxation process passing through the accessible frequency window. The relaxation times are estimated to be in the range of seconds.

Since the free carbon phase dominates the electrical behavior of the amorphous SiCN-ceramic, the adjustment of the carbon content may offer the possibility to tailor the functional properties of this material. This adjustment may be accomplished most easily by choosing the proper pyrolysis conditions or by altering the carbon content in the precursor system.

## Acknowledgements

The authors would like to thank H.-J. Kleebe for the TEM investigations.

## References

1. Verbeek, W. and Winter, G. Offenlegungsschrift 2236078 (1974).
2. Yajima, S., Okamura, K., Hayashi, J. and Omori, M., *J. Am Ceram. Soc.*, 1976, **59**, 324.
3. Mocaer, D., Pailler, R., Naslain, R., Richard, C., Pillot, J.-P., Dunogues, J., Gerardin, C. and Taulelle, F., *J. Mater. Sci.*, 1993, **28**, 2615.
4. Haluschka, C., Engel, C. and Riedel, R., *J. Eur. Ceram. Soc.*, 2000, **20**, 1365.
5. Eins, U., Bill, J. and Aldinger, F., In *Werkstoffwoche '96: Symposium 7—Materialwissenschaftliche Grundlagen*, ed. F. Aldinger and H. Mughrabi. DGM-Informationsgesellschaft Verlag, Frankfurt a. M., Germany, 1997, p. 663.
6. Lücke, J., Hacker, J., Suttor, D. and Ziegler, G., *Appl. Organomet. Chem.*, 1997, **11**, 184.
7. Böttcher, C. J. F. and Bordewijk, P., *Theory of Electric Polarisation; Vol. II. Dielectrics in Time-Dependant Fields*, 2nd edn. Elsevier Scientific Publishing Company, Amsterdam, 1978.
8. Trassl, S., Suttor, D., Motz, G., Rössler, E. and Ziegler, G., *J. Eur. Ceram. Soc.*, 2000, **20**, 215.



9. Trassl, S., Motz, G., Rössler, E. and Ziegler, G. *J. Am. Ceram. Soc.*, 2002, **85**, 239.
10. Trassl, S., Kleebe, H.-J., Störmer, H., Motz, G., Rössler, E. and Ziegler, G. *J. Am. Ceram. Soc.* 2002, **85**, 1268.
11. Wang, Y., Alsmeyer, D. C. and McCreery, R. L., *Chem. Mater.*, 1990, **2**, 557.
12. Dillon, R. O., Woollam, J. A. and Katkanant, V., *Phys. Rev.*, 1984, **B 29**, 3482.
13. Heywang, W., *Amorphe und polykristalline Halbleiter (Halbleiterelektronik Band 18)*. Springer-Verlag, Berlin, Germany, 1984.
14. Triberis, G. P. and Friedmann, L. R., *J. Phys. C: Solid State Phys.*, 1985, **18**, 2281.
15. Mott, N. F. and Davis, E. A., *Electronic Processes in Non-Crystalline Materials*, 2nd edn. Clarendon press, Oxford, 1979.
16. Emin, D., *Phys. Rev. Lett.*, 1974, **32**, 303.
17. McLachlan, D. S., Blaszkiewicz, M. and Newnham, R. E., *J. Am. Ceram. Soc.*, 1990, **73**, 2187.
18. Nathan, M. I., Smith Jr., J. E. and Tu, K. N., *J. Appl. Phys.*, 1974, **45**, 2370.
19. Tuinstra, F. and Koenig, J. L., *J. Chem. Phys.*, 1970, **53**, 1126.